Comparison of Simulated and Experimental Transport of Gases in Commercial Poly(vinyl chloride)

Pilar Tiemblo,[†] Enrique Saiz,[‡] Julio Guzmán,[†] and Evaristo Riande*[,†]

Instituto de Ciencia y Tecnología de Polímeros (CSIC), 28006 Madrid, Spain, and Departamento de Química Física, Universidad de Alcalá, Alcalá de Henares, Madri, Spain

Received November 2, 2001; Revised Manuscript Received January 29, 2002

ABSTRACT: An experimental study of the diffusion and permeability coefficients of helium, oxygen, and nitrogen in membranes prepared by solvent casting of commercial poly(vinyl chloride) (PVC) is reported. Transport parameters are very sensitive to the densification of PVC so that at 25 °C a sharp drop in the values of the permeability and solubility coefficients during the first week takes place. The variation of the transport parameters with aging time is nearly negligible after one month. Molecular dynamics methods were used to simulate a host matrix of poly(vinyl chloride) with density similar to that of the aged polymer. The application of the transition states approach to the simulation of the diffusion of gases in poly(vinyl chloride) gives values of the diffusion coefficient somewhat lower than the experimental ones for oxygen and nitrogen and higher for helium. Gas solution in poly(vinyl chloride) was simulated by means of a Monte Carlo cycle that inserts, with probability p_{in}, or removes, with probability p_{re}, particles of diffusant at randomly selected positions within the polymeric matrix. The values of the permeability coefficients calculated from the simulated diffusion and solubility coefficients are in very good agreement with the experimental results.

Introduction

The growing interest in the field of membranes has encouraged the search for polymers with optima properties for gas separation. The advances accomplished up to now are based on gas transport studies carried out on different types of membranes with the aim of finding consistent relationships between structure and transport properties of different classes of polymers.[1−4] By screening a large number of polymers with different structures, chances increase of finding specific membranes with improved gas separation properties. Some empirical rules are already being used for tailoring polymers with good discriminating transport properties. For example, it is expected that, as a result of frozenness of polymer chains in the glassy state, glassy membranes will discriminate better than rubbery membranes gas transport through them. Moreover, the information at hand suggests that glassy polymers with bulky side groups in their structure contain anomalous large cavities that facilitate gas permeability without affecting too negatively the permselectivity. These polymers have in general high glass transition temperature and therefore aging processes that might affect gas transport are not important at the temperatures of use. Polycarbonates, polysulfones, polyimides, and poly(ether imide)s are polymers commonly used in gas separation.[1−5]

Studies aimed at the simulation of transport polymers as a function of their chemical structure are still scarce.[6,7] It would be desirable to have techniques that allow the prediction of the effect of different structural features on gas transport. In principle, molecular dynamics simulations should be appropriate for this purpose. However, this technique is only suitable for the simulation of gas transport in rubbery polymers where as a result of micro-Brownian motions of the chains nonpermanent holes are continuously being created in the material into which diffusant from neighboring holes can easily jump. The situation is different in polymers in the glassy state. As a consequence of the low mobility of molecular chains in this state, a molecule of diffusant spends long time wandering in cavities until as a consequence of chains fluctuations a channel is open through which slippage of the molecule to a neighboring cavity may occur. Therefore, prohibitively large computing times would be necessary to compute the trajectories of diffusants in polymer matrices until diffusive regime is reached. Suter and co-workers[7] developed the transition states approach (TSA) to overcome this problem. The theory assumes that the molecules of gas migrate through polymer structures in a sequence of hops between local minima of the potential.

The TSA is used in this work to monitor the permeability of helium, nitrogen, and oxygen through poly(vinyl chloride) (PVC). In parallel with the simulation techniques, the permeability and diffusion coefficients of the gases in PVC are measured. By comparing simulated and experimental values of transport parameters, information assessing the suitability of the TSA for gas permeation predictions is obtained.

Experimental Part

Membranes. Poly(vinyl chloride) supplied by Rio Rodano Industries (Spain) was purified three times using tetrahydrofuran/methanol as a solvent/precipitant system. The average molecular weights of the polymer, determined by GPC, were M_w = 112 000 g/mol and M_n = 48 000 g/mol. The degree of crystallinity of commercial PVC lies in the vicinity of 7%.[8] The glass transition temperature determined at a heating rate of 10 °C/min in a Perkin-Elmer DSC-7 calorimeter was 85 °C. The stereochemical composition of PVC measured by ^{1}H NMR spectroscopy was 49% hetero, 32% syndio, and 19% iso.

PVC membranes of thickness ranging from 35 to 65 μm were prepared by casting of THF solutions on a glass plate. Traces of solvent remaining in the films were extracted with ether in a Soxhlet for 24 h, dried in a vacuum at room temperature, and kept in high vacuum until the permeation measurements were performed. Traces of solvent in the films used in the permeation measurements were not detected by IR spectroscopy.

[†] Instituto de Ciencia y Tecnología de Polímeros.
[‡] Universidad de Alcalá.

10.1021/ma011908s CCC: $22.00
Published on Web 04/12/2002

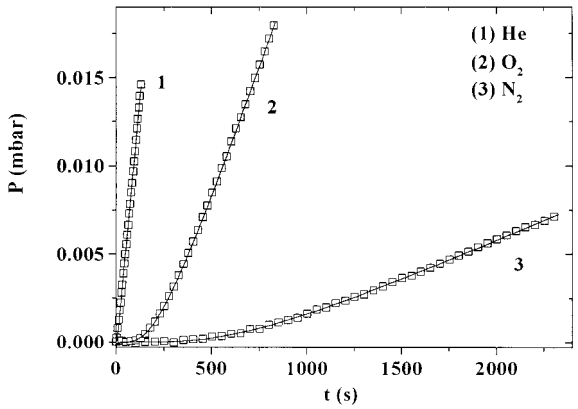

Figure 1. Variation of the pressure of gas in the downstream chamber with time under an upstream pressure of 76 cmHg. Symbols are experimental results, and the continuous line was calculated using eq 1.

An experimental device, made up of a high-pressure or upstream chamber separated from a low-pressure or downstream chamber by the PVC film, was used in the measurements of permeation. High vacuum was made in the permeation device by means of an Edwards turbomolecular pump. Gas contained in a reservoir, at 25 °C and 1 bar of pressure, was allowed to flow into the downstream chamber. The evolution of the pressure of the gas in this chamber was monitored with a MKS Baratron type 627B absolute pressure transducer working in the pressure range 10^{-4}–1 mmHg. Pressure in the upstream chamber was measured with a Gometrics transducer. Vacuum was maintained overnight in the permeation device to remove the last traces of solvent and gas in the membrane. Before performing each experiment, the inlet of air into the evacuated downstream chamber was measured as a function of time and further subtracted from the curves representing the pressure of permeant against time in the downstream chamber. All the measurements were carried out at 25 °C.

Experimental Results

Illustrative plots showing the dependence of the pressure of helium, oxygen, and nitrogen in the downstream chamber are presented in Figure 1. By using appropriate boundary conditions, the integration of Fick's second law gives the time dependence of the pressure of the gas in the downstream chamber as[9]

$$p(t) = 0.2786\,\frac{p_0 ALST}{V}\left(\frac{Dt}{L^2} - \frac{1}{6} - \frac{2}{\pi^2}\sum_{n=1}^{\infty}\frac{(-1)^n}{n^2} \times \exp\left(-\frac{Dn^2\pi^2 t}{L^2}\right)\right) \quad (1)$$

In this equation, $p(t)$ and p_0 that denote the pressures of gas in the downstream and upstream chambers, respectively, are given in cmHg, A and L that represent the area and thickness of the membrane in cm^2 and cm, respectively, the volume of the downstream chamber, V, in cm^3, and D and S are respectively the diffusion and solubility coefficients in cm^2/s and cm^3 gas (SPT)/(cm^3 polymer cmHg). Once steady-state conditions are reached, the time dependence of the pressure of the downstream chamber can be written as

$$p(t) = 0.2786\,\frac{p_0 ALST}{V}\left(\frac{Dt}{L^2} - \frac{1}{6}\right) \quad (2)$$

Plots of $p(t)$ against t in the steady state are straight lines intercepting the abscissa axis at $(D\theta/L^2) - {}^1/_6 = 0$, where θ is the time lag. Therefore, the diffusion coefficient can be obtained from the expression[10]

$$D = \frac{L^2}{6\theta} \quad (3)$$

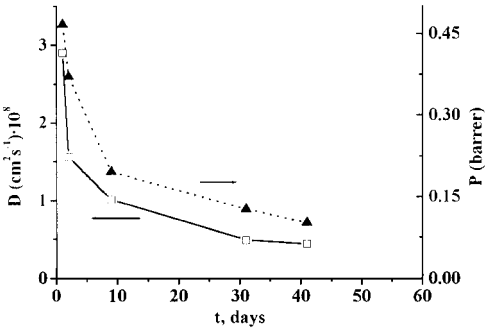

Figure 2. Variation of the permeability and diffusion coefficients of oxygen with aging time in PVC films.

By assuming that the permeability coefficient, P, is the product of the solubility coefficient times the diffusion coefficient, the value of P in barrers {1 barrer = [10^{-10} cm^3(STP) cm/(cm^2 s cmHg)]} can be obtained from eq 2, giving

$$P = 3.59\,\frac{VL}{p_0 AT}\lim_{t\to\infty}\left(\frac{\mathrm{d}p(t)}{\mathrm{d}t}\right) \quad (4)$$

where V, L, and A are given in units of the cgs system and p_0 and $p(t)$ in cmHg.

To test the reliability of the values of P and D obtained from eqs 3 and 4, these results were used in eq 1 to calculate the pressure in the downstream chamber as a function of time. As can be seen in Figure 1, the curves obtained for $p(t)$ using eq 1 fit rather well to the experimental results, indicating that the values of P and D obtained from eqs 3 and 4 are highly reliable.

There is some discrepancy among the data reported in the literature for the permeation of gases in PVC.[11−14] The discrepancy arises in part from aging processes taking place in the films used in the measurements. It has been reported that the enthalpy relaxation induced by sub-T_g annealing increases with increasing crystallization temperature, T_c, and decreases with crystallization time for PVC crystallized at a given T_c.[15] In general, aging decreases the volume excess in PVC, thus decreasing the diffusion coefficient of the permeants. Illustrative curves showing the time dependence of the permeation characteristics of membranes of PVC for oxygen are presented in Figure 2. It can be seen that both the permeability and diffusion coefficients undergo a strong decrease with time, the decrease being more marked in the first 3 days. After 1 month very small variations in both P and D were detected. Therefore, the values of the diffusion and permeation coefficients, indicated in Table 1, correspond to PVC films aged at room temperature for over 1 month.

The experimental values of the permeability coefficient, shown in Table 1, follow the trends $P(\mathrm{He}) > P(\mathrm{O_2}) > P(\mathrm{N_2})$. In fact, the permeability coefficient of helium is nearly 2 and 3 orders of magnitude higher than the permeability coefficients of oxygen and nitrogen, respectively. The high permeability of helium is due to its high diffusion coefficient that overcomes the rather low solubility of this gas in PVC. The values of the

Table 1. Experimental Values of the Diffusion Coefficient and Permeability Coefficient of Helium, Oxygen, and Nitrogen in Poly(vinyl chloride); Estimated Error on the Calculated Values of *P* Amounts to ca. ±5%

gas	$10^9 D$, cm²/s	P, barrers
He	640 ± 280	5.03
O_2	4.10 ± 0.51	0.124
N_2	0.94 ± 0.10	0.022

diffusion coefficient follow the trends $D(\mathrm{He}) > D(O_2) > D(N_2)$. The diffusion coefficient is also responsible for the high selectivity of oxygen with respect to nitrogen. Actually, the value of the permselectivity coefficient, expressed as $P(O_2)/P(N_2)$, has a value of 5.7 that compares very favorably with the permselectivity shown by other membranes for this pair of gases.

Theoretical Calculations

Force Field and Molecular Dynamics Software. The AMBER force field[16−19] was used in the present work. Coulombic interactions were computed as pairwise interactions among the partial charges assigned to every atom of the system by means of the MOPAC-AM1 procedure,[20] employing a distance-dependent dielectric constant. Cutoff distances $r_c = 11.5$ and 8 Å were used respectively for Coulombic and van der Waals interactions; i.e., interactions between atoms i and j were set to zero when their distance r_{ij} is larger than the appropriate r_c.

The DL_POLY package[21] was employed in all the MD simulations. A time step $\delta = 1$ fs (i.e., 10^{-15} s) was used for the integration of the equations of motion. The temperature of the system was kept constant by means of a Nose−Hoover thermostat[22] with a relaxation time of 500 fs. In the same way, constant pressure required for calculations performed under NpT conditions was achieved with the Nose−Hoover barostat[22] employing a relaxation time of 4000 fs. An equilibration time of 500 fs was allowed to the system to adapt to the new conditions whenever the parameters were externally modified; i.e., the size of the cubic box holding the system was changed with increments of ca. 1 Å, and the temperature was modified with increments of 50 K (see below).

Diffusion Coefficients. Calculations of the diffusion coefficients of the diffusant particles (i.e., He atoms, O_2 or N_2 molecules) within the polymeric membrane were carried out employing the transition state approach (TSA),[7,23−31] whose main assumption is that the atoms on the polymeric membrane have fixed main positions. Oscillations over those main positions are however allowed with a root-mean-square value Δ, which is customarily referred to as smearing factor. Thus, the probability of finding atom i of the polymeric matrix at a distance δ of its main position does not depend on the relative orientation of the instantaneous and main positions of the atom, and it is given by

$$W_i(\delta) \sim \exp\left(-\frac{\delta^2}{2\Delta^2}\right) \qquad (5)$$

The smearing factor Δ accounts for the difference between thermal linear motion of the diffusant particle and the fast mobility of the atoms in the polymeric host matrix due to bond lengths vibrations and angle bending. The exact determination of this parameter is virtually impossible at the moment. However, rough estimations[27,28,31] suggest a value of ca. 0.3−0.4 Å. In the present work, we shall use a value $\Delta = 0.3$ Å which has already been employed for many other systems,[27−31] producing good agreement between experimental and calculated values of the diffusion coefficient.

A second hypothesis is required when the diffusant particles are molecules instead of single atoms. It consists of assuming that the rotation of the diffusant molecule is much faster than its linear translation and allows the separation among rotational and translational variables.[7,23−31] Averaging can then be performed over all the allowed rotations for each position of the molecule.

The application of TSA requires then three steps that will be described in the next paragraphs, namely, (a) preparation of the host polymeric matrix determining the main positions of all the atoms on the matrix, (b) evaluation of the interactions between the diffusant guest molecule and the host matrix that determine the probability of finding the guest particle at each point of the host matrix, and (c) random walk of the diffusant throughout the matrix.

(a) Preparation of the Polymeric Host Matrix. The protocol used to prepare the polymeric host matrix was similar to those previously employed.[27−31] Thus, the basic polymeric chain was a H-terminated oligomer containing 90 repeating units of PVC with ca. 40% content of meso units and random placement of meso and racemic centers. Four such oligomers (i.e., 2168 atoms in total) were packed into a cubic box having periodic boundary conditions (PBC) and a box side length $L = 29.99$ Å in order to reproduce the experimental density of 1.385 g cm^{-3} corresponding to aged PVC. The system was first built within a much larger box with twice the final desired value of L in order to avoid extremely high energies that would be produced if the atoms were initially placed too close to each other. Those interactions may render inaccurate any procedure of energy minimization employed afterward. A MD simulation at $T = 500$ K was then initiated during which the side length of the cubic box was decreased toward the desired final value of $L = 29.99$ Å. Once the correct volume was reached, the sample was submitted to a series of simulated annealings during which the system was repeatedly warmed and cooled between 50 and 500 K under NVT conditions. Finally, the sample was warmed from 50 to 300 K under NpT and then allowed to equilibrate at this temperature, still under NpT conditions, until the density remained constant that occurs at ca. 50 000 ns. The matrix thus produced has a box side length $L = 30.5$ Å (and therefore a density of 1.32 g cm^{-3}, in good agreement with the experimental value) and will be employed in all the following sections. The position of each polymeric atom, for instance atom i, in this equilibrated matrix is the "main" or "equilibrium" position for atoms i and determines the main distance R_i from this atom to a diffusant particle placed at a given grid point (see below). Analysis of the rotational angles over skeletal CC−CC bonds indicates that they adopt the three staggered positions, namely trans ($\phi \approx 180°$) and the two gauche ($\phi \approx \pm 60°$), with population fractions of ca. $p_{\mathrm{trans}} \approx 0.58$ and $p_{\mathrm{gauche}} \approx 0.21$.

(b) Interactions between the Diffusant Particle and the Host Polymer Atoms. Let us consider a diffusant particle, either a single atom, as represented in the top part of Figure 3, or a diatomic AB molecule

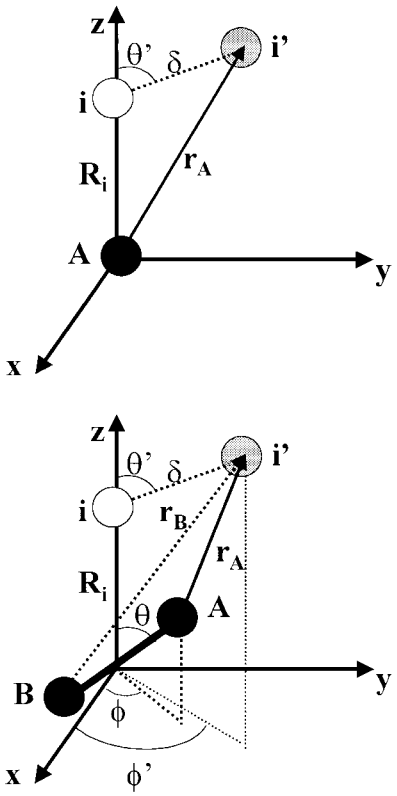

Figure 3. A rough sketch illustrating the interaction of atom *i* of the polymeric matrix with the diffusant particle which is a single atom in the top panel and a diatomic AB molecule in the bottom part. Arbitrary coordinate systems are centered at the diffusant atom or the center of the A−B bond with the *z* axis in the direction of the equilibrium position of matrix atom *i*.

that is shown in the bottom part of the same figure. According to the TSA,[7,23−31] the polymer atoms are fixed at main positions which for atom *i* on the matrix is represented by the open circles in Figure 3. However, since the polymer atoms are allowed to oscillate, the actual position of atom *i* at a given moment may be *i*′, represented by the gray circles in Figure 3. The interaction between the diffusant particle and the polymer atom *i* depends on the interatomic distances r_A or r_A and r_B respectively for atoms or molecules. These distances may be written as a function of the equilibrium distance R_i, the displacement δ produced by the oscillation and the appropriate orientational angles. Consequently, the interaction between the diffusant particle and the atom *i* of the polymer is given by

$$\text{atom:} \quad E_i(r_A) = E_i(R_i,\delta,\theta')$$

$$\text{molecule:} \quad E_i(r_A,r_B) = E_i(R_i,\delta,\theta,\phi,\theta',\phi') \qquad (6)$$

Boltzmann factors of these energies may be integrated over δ and the orientational angles to compute the partition function $Z_i(R_i)$ and the free energy of the interaction as a function of the equilibrium distance between the diffusant particle and the polymer atom *i*:

$$F_i(R_i) = -kT\ln[Z_i(R_i)] \qquad (7)$$

where the subscript indicates that only the polymer atom *i* is considered. Both the partition function and the free energy depend only on equilibrium distances R_i among diffusant and polymer atom. The only noticeable difference between single atoms and diatomic molecules as diffusants is the number of orientational parameters included in eq 6 and the consequent difference in the computational time required for performing the integration.

Next, the cubic box containing the polymer matrix is gridded by dividing each side of the cube into $G = 100$ intervals, each one of length L/G. A total of $G^3 = 10^6$ grid points, each one having a volume of $(L/G)^3$, are thus obtained. The diffusant particle is placed successively at each one of these grid points, and the interaction between the diffusant particle and all the atoms on the matrix is computed by adding the interactions with every atom. Thus, the interaction energy at grid point m is

$$F_m = \sum_{\text{atoms}} F_i(R_i) = -kT \sum_{\text{atoms}} \ln[Z_i(R_i)] \qquad (8)$$

where the sums are performed over all the atoms on the polymer matrix. The result is then a set of one value of energy for each grid point. These values of F_m will be used in the next sections. For instance, the partition function for the whole matrix may be evaluated as

$$Z_{\text{matrix}} = \sum_{\text{grid}} \exp(-F_m/kT) \qquad (9)$$

where the sum is over all the grid points of the matrix.

(c) Random Walk of the Diffusant throughout the Matrix. As usual, the diffusion of the particle throughout the polymer matrix is simulated by a random walk among sites that are defined as the areas where the interaction energy is a local minima.[7,23−31] The position and extent of the sites contained in the matrix were determined by a steepest descendent algorithm starting at each grid point and ending at the site where the starting point belongs. The crest surface between neighbor sites α and β is formed by the loci of grid points *i* meeting the condition that point *i* belongs to site α while at least one among its immediate neighbors belongs to site β. Partition functions for each site Z_α, and for the crest surface separating neighbor sites α and β $Z_{\alpha\beta}$, can be computed through expressions similar to eq 9 with the sums expanding over the grid points belonging to site α (for Z_α) or to the crest surface separating α and β (for $Z_{\alpha\beta}$). The rate of diffusant transitions from site α to a neighbor site β is given by

$$R_{\alpha\beta} = W_{\alpha\beta}\left(\frac{kT}{8\pi m}\right)^{1/2}\frac{Z_{\alpha\beta}}{Z_\alpha} \qquad (10)$$

where *m* is the mass of the diffusant particle and $W_{\alpha\beta}$ a dimensionless parameter that was taken to be zero when the crest surface is smaller than the cross section of the diffusant particle and unity otherwise. The role of $W_{\alpha\beta}$ is to eliminate the transitions when the channel connecting the two sites is too narrow as to allow the passage of one diffusant particle. The cross section of the diffusant particles were taken as that of spheres having the van der Waals radius in the case of single atoms and the sum of one van der Waals radius plus half the bond length in the case of diatomic molecules.[32]

The probability for the $\alpha \rightarrow \beta$ transition is then

$$p_{\alpha\beta} = \tau_\alpha R_{\alpha\beta} \qquad (11)$$

with τ_α being the mean residence time for the guest

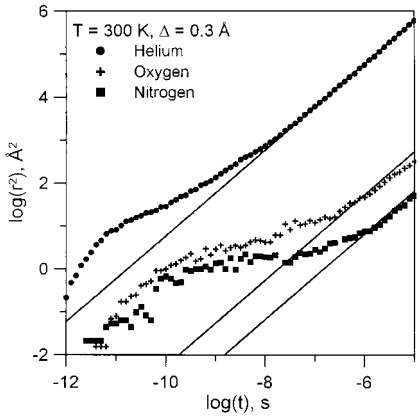

Figure 4. Double-logarithmic plot of the time dependence of the squared displacement r^2 of the three gases studied within a polymeric matrix of PVC. Calculations were performed according to the TSA scheme at 300 K with a smearing factor $\Delta = 0.3$ Å. Fittings of the diffusive region employed for the evaluation of the diffusion coefficient D are shown by solid lines.

atom in site α:

$$\tau_\alpha = \frac{1}{\sum_{\beta=1}^{n} R_{\alpha\beta}} \tag{12}$$

where the sum is performed over all the n sites that are neighbors of site α.

The diffusion process is then simulated by a series of jumps from one initial site α to a site β that is randomly selected among the neighbors of site α. The jump is assumed to require a time equal to τ_α to take place.[7,23−31] Site β is then taken as initial position for the second jump to one of its neighbors, for instance γ, and the process is continued until the accumulated time equals a predetermined value, which in this work was set to 10^{-5} s. The initial site for the first jump is randomly chosen, and the displacement of the molecule from this starting position $\mathbf{r}^2$ is recorded as a function of time. All the results shown below represent averages over 500 independently generated trajectories of the diffusant particle throughout the matrix.

Figure 4 shows a double-logarithmic plot of the squared displacement $\mathbf{r}^2$ as a function of time for the three diffusant particles studied computed at 300 K with a value $\Delta = 0.3$ Å for the smearing factor.[27−31] As can be seen in Figure 4, the displacement is strongly time sensitive. However, a diffusive regime is eventually reached in which $\mathbf{r}^2$ varies linearly with time.

Solubility. The solution of the diffusant particles into the polymeric membrane was simulated by a procedure that, in many aspects, could be regarded as a variation of the Widom's test particle insertion method.[33,34] Thus, the first step consists of calculating the total energy of interaction between all the polymeric atoms contained in the matrix and the diffusant particle when it is placed at different positions within the matrix. In fact, this energy was computed in the preceding sections, and it is given by eq 8 as F_m for grid point m. However, instead of inserting test particles into the system and compute the excess chemical potential, we employ the F_m energy to compute the probability for inserting or removing an actual diffusant molecule at every grid point within the matrix and employ a Monte Carlo simulation that tries to insert or remove particles at randomly selected grid positions. Once the simulation reaches the convergence limit, the number of diffusant molecules inserted into the system gives the actual concentration of the gas into the polymeric matrix. It should be pointed out that the values of F_m were computed according to the postulates of TSA; i.e., the atoms of the polymeric matrix have fixed main positions but are allowed to fluctuate with a smearing factor $\Delta = 0.3$ Å. Moreover, different orientations of the diffusant molecules are taken into account during the evaluation of F_m. Consequently, these energies are in fact averages over many different configurations of the system, and the sampling procedure is much more efficient than if they were computed for an absolutely rigid matrix.

The probabilities of inserting and removing a diffusant particle at a given grid point, p_{in} and p_{re}, were evaluated as the product of three factors. The first factor depends on the pressure p and temperature T, at which the solution process is performed. The second one depends on the energy of interaction between the diffusant particle and the polymer host matrix, F_m. The third factor depends on the volume of the diffusant particle.

The number of particles of gas at pressure p and temperature T allowed to fill up an empty volume V is given by

$$N = \frac{pV}{kT} \tag{13}$$

This process would be easily simulated with a Monte Carlo sampling employing the following probabilities:

$$p'_{\text{in}} = \frac{pV}{2nkT} \qquad p'_{\text{re}} = \frac{(n-1)kT}{2pV} \tag{14}$$

where n represents the number of particles actually contained in the system at the moment that the attempt to insert or remove one particle is performed. These probabilities are identical over all the volume of the matrix so that they do not depend on the location of the point at which the insertion or removal is attempted.

According to eq 14, when the system contains $n = N$ particles, i.e., the equilibrium value given by eq 13, the probability of inserting a new particle would be identical to the probability of removing one particle when the system contains $n = N + 1$ particles. Consequently, the transitions $N \rightleftarrows N + 1$ will have the same probability, and the number of particles should be kept constant. However, when $n < N$, $p'_{\text{in}} > p'_{\text{re}}$ and the insertion attempts would be more efficient than the removal ones and the number of particles contained in the system will increase. On the contrary, $p'_{\text{re}} > p'_{\text{in}}$ when $n > N$ and the number of the particles contained in the system will decrease as the MC cycles go on.

An important difficulty for this scheme is that the volume of the cubic box employed in the preceding sections is too small as to allow a reasonable MC sampling. Thus, with box sides on the order of $L \approx 30$ Å, i.e., $V \approx 2.7 \times 10^{-20}$ cm^3, the equilibrium number of particles under STP conditions would be ca. $N \approx 0.7$. To avoid this inconvenience, we set up an assemble of $(N_{\text{box}})^3$ boxes identical to the one employed in the preceding sections and packed into a cube with side

LN_{box}. Equation 14 could then be rewritten as

$$p'_{in} = \frac{pL^3 N_{box}^3}{2nkT} \qquad p'_{re} = \frac{(n-1)kT}{2pL^3 N_{box}^3} \tag{15}$$

The value of N_{box} can then be employed as a parameter that controls the amount of sampled volume and the total number of molecules that are fitted into it, ensuring that this number is large enough as to warrant a statistical sampling. For instance, taking $N_{box} = 5$, the sampled volume should contain ca. $N \approx 90$ gas particles under STP. Some test calculations performed with different values of pressure and temperature proved that the equilibrium values of N are reached with errors of ca. 2% after a few thousand MC cycles.

However, since the volume V contains the polymeric matrix that interacts with the solute molecule, the probability of finding a particle in a given position i within the matrix will depend on the potential energy F_i that the solute particle would have when placed at position i. Thus, the probabilities of inserting a particle into position i, at fixed values of pressure and temperature, would be proportional to a Boltzmann factor of F_m:

$$p''_{in} = \exp(-F_m/kT) \qquad p''_{re} = \frac{1}{\exp(-F_m/kT)} \tag{16}$$

According to eq 16, if F_m had the same value for all the grid points, $p''_{in} = p''_{re}$ and the molecules of diffusant would be inserted with the same probability all over the matrix, in the same way that if the volume was empty. However, in the actual situation in which F_m changes noticeably over the matrix, insertions will be more efficient than removals in grid points having $F_m < 0$ while the opposite would happen in the case of grid points with $F_m > 0$.

The third factor to be considered in the formulation of the probabilities concerns the volume of the diffusant molecule and arises from the fact that one diffusant molecule occupies many grid positions. In fact, if the volume of the diffusant is V_{molec} while the volume of the matrix is L^3 and it has been divided into G^3 grid points (see above), the number of positions occupied by a single diffusant molecule would be[35]

$$g = V_{molec}(G/L)^3 \tag{17}$$

and the matrix would be completely filled up with diffusant molecules when insertion has succeeded in 1 among each g grid positions. Consequently, we define the third factor as

$$p'''_{in} = \frac{L^3}{V_{molec}G^3} \qquad p'''_{re} = \frac{V_{molec}G^3}{L^3} \tag{18}$$

The actual probabilities can be obtained by multiplication of the three factors defined by eqs 15, 16, and 18 as

$$p_{in} = \frac{pL^6 N_{box}^3}{2nkTV_{molec}G^3}\exp(-F_m/kT)$$

$$p_{re} = \frac{(n-1)kTV_{molec}G^3}{2pL^6 N_{box}^3 \exp(-F_m/kT)} \tag{19}$$

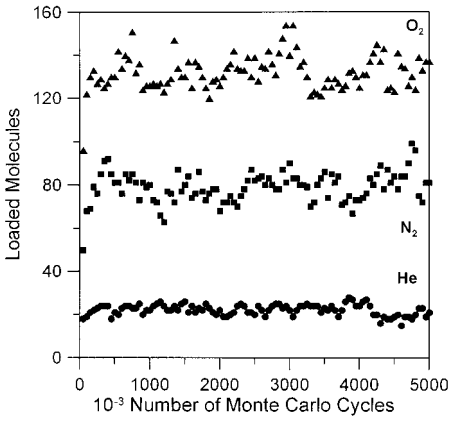

Figure 5. Number of molecules of gas inserted in the polymeric matrix as a function of the Monte Carlo steps. Calculation were performed at $T = 300$ K, $p = 76$ cmHg, and $N_{box} = 5$. The asymptotic limit of this number is transformed into gas concentration by means of eq 21.

The normalization of p_{in} and p_{re} leads to

$$p^0_{in} = \frac{p_{in}}{p_{in} + p_{re}} \qquad p^0_{re} = \frac{p_{re}}{p_{in} + p_{re}} \tag{20}$$

The MC simulation consisted in series of 5×10^6 cycles. At each cycle, a grid position m within the polymeric matrix was randomly selected. The value of the energy at that position F_m, together with the number of particles previously loaded into the system n, allows the evaluation of the probabilities of insertion p^0_{in} and removal p^0_{re} at grid point m according to eqs 19 and 20. Then, a random number x within the interval 0−1 was generated and compared with p^0_{in}. When $x \leq p^0_{in}$, an attempt to insert a new particle into position m was performed; otherwise, i.e., when $x > p^0_{in}$, removal of one particle from position n was attempted.

An insertion attempt was successful; i.e., a new particle was inserted with its center of masses located at position m when none of the n particles previously loaded into the system has its center of masses within a distance smaller than a molecular diameter from position m. In other words, when the new loaded molecule would not overlap with any of the previously loaded particles. However, insertion attempts that would place the new molecule overlapping with a previously loaded one are very infrequent because the number of molecules loaded into the matrix is much smaller than what would be allowed by the ratio among the volumes of the matrix and the molecule. Consequently, most of the insertion attempts take place at well-separated points. For this reason, no interactions among molecules of solute were considered when computing the exponential of energy appearing in eqs 16 and 19. On the other hand, a removal attempt was successful; i.e., one particle was removed from the system when its center of mass lies within a distance smaller than the molecular radius from the tested position. In other words, when the tested position is one among the g grid positions occupied by one of the molecules contained in the system. Of course, failed attempts to either insert or remove particles leave the system unchanged.

Figure 5 shows the number n of molecules of diffusant gas loaded into the polymeric matrix as a function of

Table 2. Summary of Calculated Values Computed at 300 K for the Three Diffusant Particles within a PVC Polymeric Matrix[a]

		parameters of eq 23			10^3S at	
solute	10^9D	10^3k_D	C_H	b	76 cm(Hg)	P
He	980	1.6	0.14	0.052	3.1	30
O_2	0.92	4.9	1.2	0.058	18	0.17
N_2	0.12	2.8	0.72	0.081	11	0.013

[a] Units: D in cm^2 s^{-1}; k_D and S in cm^3 (STP) cm^{-3} (cmHg)$^{-1}$; C_H in cm^3 (STP) cm^{-3}; b in (cmHg)$^{-1}$ and P in barrers.

the number of MC cycles employed. Calculations were performed at 300 K and $p = 76$ cmHg for the three gases studied here. The value of the N_{box} parameter that controls the actual size of the sampled volume was set to 5 for the three gases. As Figure 5 indicates, the value of n reaches a roughly constant value after ca. 5×10^5 MC cycles. All the results shown below are averages over 50 independent simulations, each one of then containing 5×10^6 MC cycles.

Assuming that the equilibrium is reached when the matrix contains n molecules of solute, this concentration can be transformed into the desired units of cm^3 (STP) cm^{-3} by means of the relationship

$$c = 3.719 \times 10^4 \frac{n}{(N_{box}L)^3} \tag{21}$$

where L represents the length, in angstroms, of the primary cubic box and $N_{box}L$ is the side of the cube actually employed in this simulation.

Results and Discussion

The diffusive region in the log r^2 vs log t plots shown in Figure 4 was fitted to a straight line, and the diffusion coefficient was then computed according to Einstein's relationship:

$$D = \frac{1}{6}\lim_{t\to\infty}\left\{\frac{\partial}{\partial t}\langle(\mathbf{r}(t) - \mathbf{r}(0))^2\rangle\right\} \tag{22}$$

The values of the diffusion coefficient thus obtained are summarized in the second column of Table 2. Comparison of these theoretical results with the experimental ones shown in Table 1 indicates that the calculation overestimates the value of D for He while it underestimates the values of the two diatomic molecules. However, it correctly predicts the trend D(He) $\gg D(O_2) > D(N_2)$.

Figure 6 shows the values of solubility as a function of pressure for the three gases studied. They were computed at $T = 300$ K as the average among the results obtained with 50 independently generated Monte Carlo runs. Vertical bars on this figure represent standard deviations on the averages. The shape of the curves concentration vs pressure is similar to those observed in the pressure dependence of the concentration in glassy polymers. The interpretation of the sorption process in glassy matrices has customarily been made by means of the dual mode model.[36] The model assumes that the matrix is made up of a continuous phase in which microvoids that account for the excess volume of the glassy state are dispersed. Absorption processes take place in the continuous phase that obeys Henry's law whereas adsorption processes occur in the microvoids. Accordingly,

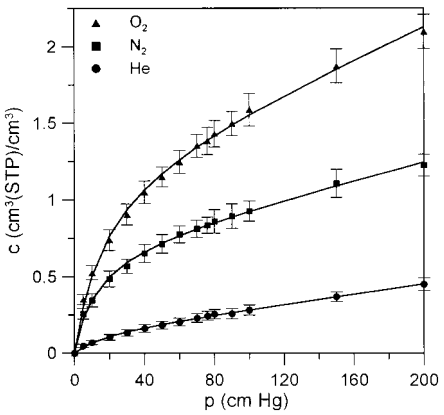

Figure 6. Concentration inside the polymeric matrix of the three gases studied as a function of pressure. Calculations were performed at $T = 300$ K, and each point represents the average over 50 independently generated Monte Carlo runs performed as indicated in the text. Vertical bars indicate standard deviations of the averages. Solid lines represents fits to eq 23.

$$c = k_D p + \frac{C_H b p}{1 + bp} \tag{23}$$

where k_D is the absorption constant in Henry sites, C_H is the gas concentration in Langmuir sites, and b is an affinity parameter between the gas and the matrix. Fitting of eq 23 to the experimental results, shown as solid lines in Figure 6, gives the values of the dual mode model parameters collected in columns three, four, and five of Table 2. The solubility coefficient, S, defined as the ratio between the gas concentration c and the pressure, can then be computed at pressure p as

$$S(p) = k_D + \frac{C_H b}{1 + bp} \tag{24}$$

The values of the solubility coefficient at $p = 76$ cmHg, shown in column six of Table 2, in conjunction with those simulated for the diffusion coefficient, give the permeability coefficients presented in the last column of Table 2. It can be seen that there exists a rather good agreement between the experimental and simulated values of the permeability coefficients.

In previous publications,[7,23−31] the solubility coefficient of the diffusant gas in the host matrix was evaluated using the following approach:

$$S = \frac{1}{k_B T V}\int_V \exp\left(-\frac{E}{RT}\right) \mathrm{d}V = \frac{1}{k_B T}\left\langle\frac{Z}{G}\right\rangle \tag{25}$$

where V is the volume of the polymer matrix and G the number of grid points employed to compute the partition function Z. The values of 10^3S, in cm^3 (STP)/(cm^3 cmHg), obtained by means of eq 25 are 2.02, 86.3, and 131.7 for He, N_2, and O_2, respectively. Agreement with the results obtained by the method outlined above is good for He and quite poor in the case of the two diatomic molecules. Moreover, the solubility coefficient computed by using eq 25 is independent of the pressure, and therefore this expression is only of limited value to determine the solubility of gases in glassy matrices. The use of probabilities for insertion and removal of solute particles explained in detail above seems to outline a promising way of simulating the solubility of gases in host matrices as a function of the concentration.

Conclusions

The transport properties of gases in glassy polymers at temperature relatively close to the glass transition temperature decrease with time as a consequence of the increase of densification caused by aging processes. In these cases, the transport parameters should be obtained in systems kept at the temperature of interest for a long time.

Simulations of the diffusion coefficient of oxygen, nitrogen, and helium in poly(vinyl chloride) performed with the transition states approach give values of D that are in fair agreement with the experimental results. This analysis and others carried out in other polymer suggest that the TSA can be a useful tool to predict gas transport in glassy membranes as a function of the chemical structure.

A method is described that may allow a realistic prediction of the solubility of gases in polymers as a function of structure. The method is a step ahead of those previously used since it allows the calculation of the gas concentration in a host matrix as a function of pressure.

Acknowledgment. This work was supported by the CAM through Grant BIO-009-2000 and the DGESIC through Grants PB97-0778, BQU2001-1158 and MAT-1999-1127-C04-01.

References and Notes

(1) Kesting, R. E.; Fritzsche, A. K. *Polymeric Gas Separation Membranes*; Wiley-Interscience: New York, 1993.
(2) Ohya, H.; Kudryavtsev, V. V.; Semenova, S. I. *Polyimide Membranes*; Gordon and Breach Publishers: Tokyo, 1996.
(3) Koros, W. J.; Fleming, G. K. *J. Membr. Sci.* **1993**, *83*, 1.
(4) Stern, S. A. *J. Membr. Sci.* **1994**, *94*, 1.
(5) Al-Masri, M.; Kricheldorf, H. R.; Fritsch, D. *Macromolecules* **1999**, *32*, 7853.
(6) Müller-Plathe, F.; Rogers, S. C.; van Gunsteren, W. F. *J. Chem. Phys.* **1993**, *98*, 9895.
(7) Gusev, A. A.; Müller-Plathe, F.; van Gunsteren, W. F.; Suter, U. W. *Adv. Polym. Sci.* **1994**, *116*, 207.
(8) Summers, J. W. *J. Vinyl Technol.* **1981**, *3*, 107.
(9) Crank, J. *The Mathematics of Diffusion*; Oxford University Press: Oxford, 1975.
(10) Barrer, R. M. *Trans. Faraday Soc.* **1939**, *35*, 628.
(11) Pauly, S. *Permeability and Diffusion Data* in *Polymer Handbook*, 4th ed.; Bandrup, J., Immergut, E. H., Grulke, A. E. J., Eds.; Wiley: New York, 1999; p VI/543-69.
(12) El-Hibri, J.; Paul, D. R. *J. Appl. Polym. Sci.* **1985**, *30*, 3649.
(13) Tikhomirov, B. P.; Hofenberg, H. B.; Stannet, V. T.; Williams, J. L. *Makromol. Chem.* **1968**, *118*, 177.
(14) Tiemblo, P.; Guzmán, J.; Riande, E.; Mijangos, C.; Reinecke, H. *Polymer* **2001**, *42*, 4817.
(15) Tsitsilianis, C.; Tsapatsis, M.; Economou, C. *Polymer* **1989**, *30*, 1861.
(16) Weiner, S. J.; Kollman, P. A.; Nguyen, D. T.; Case, D. A.; Singh, U. C.; Ghio, C.; Alagona, G.; Profeta, S.; Weiner, P. J. *J. Am. Chem. Soc.* **1984**, *106*, 765.
(17) Weiner; S. J.; Kollman, P. A.; Nguyen, D. T.; Case, D. A. *J. Comput. Chem.* **1986**, *7*, 230.
(18) Homans, S. W. *Biochemistry* **1990**, *29*, 2110.
(19) Cornell, W. D.; Cieplak, P.; Bayly, C. L.; Gould, I. R.; Merz, K. M.; Ferguson, D. M. D.; Spellmeyer, C.; Fox, T.; Caldwell, J. W.; Kollman, P. A. *J. Am. Chem. Soc.* **1995**, *117*, 5179.
(20) MOPAC, *Quantum Chemistry Program Exchange*, Department of Chemistry, Indiana University, Bloomington, IN.
(21) Forester, T. R.; Smith, W. *DL_POLY* (Ver. 2.10), Daresbury Laboratory, Daresbury, Warrington WA4 4AD, England.
(22) Allen, M. P.; Tildesley, D. J. *Computer Simulation of Liquids*; Clarendon: Oxford, 1987.
(23) Gusev, A. A.; Suter, U. W.; Moll, D. J. *Macromolecules* **1995**, *28*, 2582.
(24) Gusev, A. A.; Arizzi, S.; Suter, U. W.; Moll, D. J. *J. Chem. Phys.* **1993**, *99*, 2221.
(25) Gusev, A. A.; Suter, U. W. *J. Chem. Phys.* **1993**, *99*, 2228.
(26) Gusev, A. A.; Suter, U. W. *J. Comput.-Aided Mater. Design* **1993**, *1*, 63.
(27) Laguna, M. F.; Guzmán; J.; Riande, E.; Saiz, E. *Macromolecules* **1998**, *31*, 7488.
(28) Laguna, M. F.; Guzmán, J.; Saiz, E.; Riande, E. *J. Chem. Phys.* **1999**, *110*, 3200.
(29) López-González, M.; Saiz, E.; Guzmán, J.; Riande, E. *J. Chem. Phys.* **2001**, *115*, 6728.
(30) López-González, M.; Saiz, E.; Guzmán, J.; Riande, E. *Macromolecules* **2001**, *34*, 4999.
(31) López-González, M.; Saiz, E.; Riande, E.; Guzmán, J. *Polymer* **2002**, *43*, 409.
(32) This definition of the cross section for a diatomic molecule is consistent with the assumption that its rotation is much faster than the translation.
(33) Widom, B. *J. Chem. Phys.* **1963**, *39*, 2808.
(34) Cuthbert, T. R.; Wagner, N. J.; Paulaitis, M. E. *Macromolecules* **1997**, *30*, 3058.
(35) It is important to realize that the number of grid point occupied by one molecule of diffusant does not depend on N_{box} since the total volume of the system would be $V = (LN_{box})^3$ while the total number of grid positions is $(GN_{box})^3$ so that the ratio grid positions to volume is independent of N_{box}.
(36) Vieth, W. R.; Sladek, K. J. *J. Colloid Sci.* **1965**, *20*, 1014.

MA011908S